

Cancer Cell, Volume 29

Supplemental Information

Inhibition of Dopamine Receptor D4 Impedes

Autophagic Flux, Proliferation, and Survival

of Glioblastoma Stem Cells

Sonam Dolma, Hayden J. Selvadurai, Xiaoyang Lan, Lilian Lee, Michelle Kushida, Veronique Voisin, Heather Whetstone, Milly So, Tzvi Aviv, Nicole Park, Xueming Zhu, ChangJiang Xu, Renee Head, Katherine J. Rowland, Mark Bernstein, Ian D. Clarke, Gary Bader, Lea Harrington, John H. Brumell, Mike Tyers, and Peter B. Dirks

SUPPLEMENTAL DATA

Table S1, related to Figure 1

<u>Drug name</u>	<u>Fold selectivity^a</u>	<u>Class</u>	<u>Activity</u>
5-Iodotubercidin	6	Adenosine	Adenosine kinase inhibitor
Ifenprodil tartrate	16	Glutamatergic/ Adrenergics	NMDA receptor antagonist/Alpha 1 adrenergic antagonist
RS 17053 HCl	4	Adrenergics	Alpha 1A adrenergic antagonist
(±)-Isoproterenol HCl	Not active	Adrenergics	Beta adrenergic agonist
(-)-Cyanopindolol hemifumarate	Not active	Adrenergics	Beta adrenergic antagonist
Ivermectin	16	Cholinergics	Allosteric modulator of alpha 7 nicotinic receptor
MG-624	64	Cholinergics	Alpha 7 nicotinic antagonist
(-)-N-Phenylcarbamoylseroline	Not active	Cholinergics	Choline acetyltransferase inhibitor
(±)-Tropanyl-2-(4-chlorophenoxy)butanoate	32	Cholinergics	Stimulates acetylcholine release
R(+)-SKF-81297	0	Dopaminergics	Dopamine receptor D1 agonist
R(-) Propylnorapomorphine HCl	2	Dopaminergics	Dopamine receptor D2 agonist
L-741,742	>8	Dopaminergics	Dopamine receptor D4 antagonist
Fluphenazine 2HCl	4	Dopaminergics	Dopamine antagonist
Thioridazine HCl	6	Dopaminergics	Dopamine antagonist
3-a-[(4-Chlorophenyl) phenylmethoxy] tropane HCl	2	Dopaminergics	Dopamine uptake inhibitor
GBR-12909	4	Dopaminergics	Dopamine uptake inhibitor
GBR 13069 2HCl	4	Dopaminergics	Dopamine uptake inhibitor
GBR 12935 2HCl	4	Dopaminergics	Dopamine uptake inhibitor
PNU 96415E	>16	Dopaminergics	Dopamine receptor D4 antagonist
Astemizole	0	Histaminergics	H1 Histamine antagonist
N,N-Diethyl-2-[4-(phenylmethyl)phenoxy]ethanamine	>64	Histaminergics	Histamine antagonist
BNTX maleate	2	Opoids	Delta 1 opioid antagonist
LY-165,163	>16	Serotonergics	Serotonin 5-HT 1A agonist
SB 216641 HCl	2	Serotonergics	Serotonin 5-HT 1B antagonist
MDL-72222	8	Serotonergics	Serotonin 5-HT 3 antagonist

Tropanyl 3,5-dimethylbenzoate	>32	Serotonergics	Serotonin 5-HT 3 antagonist
RS 39604 HCl	2	Serotonergics	Serotonin 5-HT 4 antagonist
1-Methyl-4-[2-(2-naphthyl)-ethenyl]-pyridinium iodide	6	Sigma receptor	Sigma receptor ligand
cis-(±)-N-Methyl-N-[2-(3,4-dichlorophenyl)ethyl]-2-(1-pyrrolidinyl)cyclohexamine 2HBr ^b	16	Sigma receptor	Sigma receptor ligand

^a. Fold selectivity = IC₅₀ of BJ / IC₅₀ of NS or GNS with lowest number.

“>” Indicates IC₅₀ not seen even at highest concentration tested (50 μM) in BJ thus may be more selective than the number indicated.

^b. Not available for further retest

Table S2, related to Figure 1

	BJ	U20S	Daoy	C8-D1A	hf5281	hf5205	hf7450	GlINS1	G144	G380	Fold selectivity (NS selective)^a	Fold selectivity (GNS selective)^b
Ifenprodil tartrate	50	50	50	25	12.5	12.5	3.12	3.12	3.12	0.39	128	8
L-741,742	>50	50	>50	12.5	12.5	12.5	12.5	6.25	6.25	1.56	>32	8
PNU 96415E	>50	>50	>50	>50	25	25	12.5	6.25	3.12	1.56	>32	8
LY-165,163	>50	>50	>50	>50	3.12	6.25	3.12	3.12	6.25	3.12	>16	
MDL-72222	50	50	>50	12.5	12.5	6.25	6.25	6.25	6.25	6.25	8	
Tropanyl 3,5 dimethylbenzoate	>50	>50	50	25	12.5	1.56	3.12	1.56	1.56	3.12	>32	
N,N-Diethyl-2-[4-(phenylmethyl)phenoxy]ethanamine	>50	50	25	25	0.78	1.56	3.12	0.78	0.78	1.56	>64	
(±)-Tropanyl-2-(4-chlorophenoxy)butanoate	50	50	25	12.5	3.12	6.25	3.12	3.12	1.56	0.39	128	
MG-624	25	25	25	6.25	1.56	0.78	0.39	0.78	0.39	3.12	64	
Ivermectin	12.5	12.5	12.5	12.5	0.78	3.12	1.56	1.56	1.56	1.56	16	

^a. NS selective = IC₅₀ of BJ / IC₅₀ of NS or GNS with lowest number

^b. GNS selective = IC₅₀ of any NS with highest number / IC₅₀ of GNS with lowest number

“>” Indicates IC₅₀ not seen even at highest concentration tested (50 μM) thus may be more selective than the number indicated.

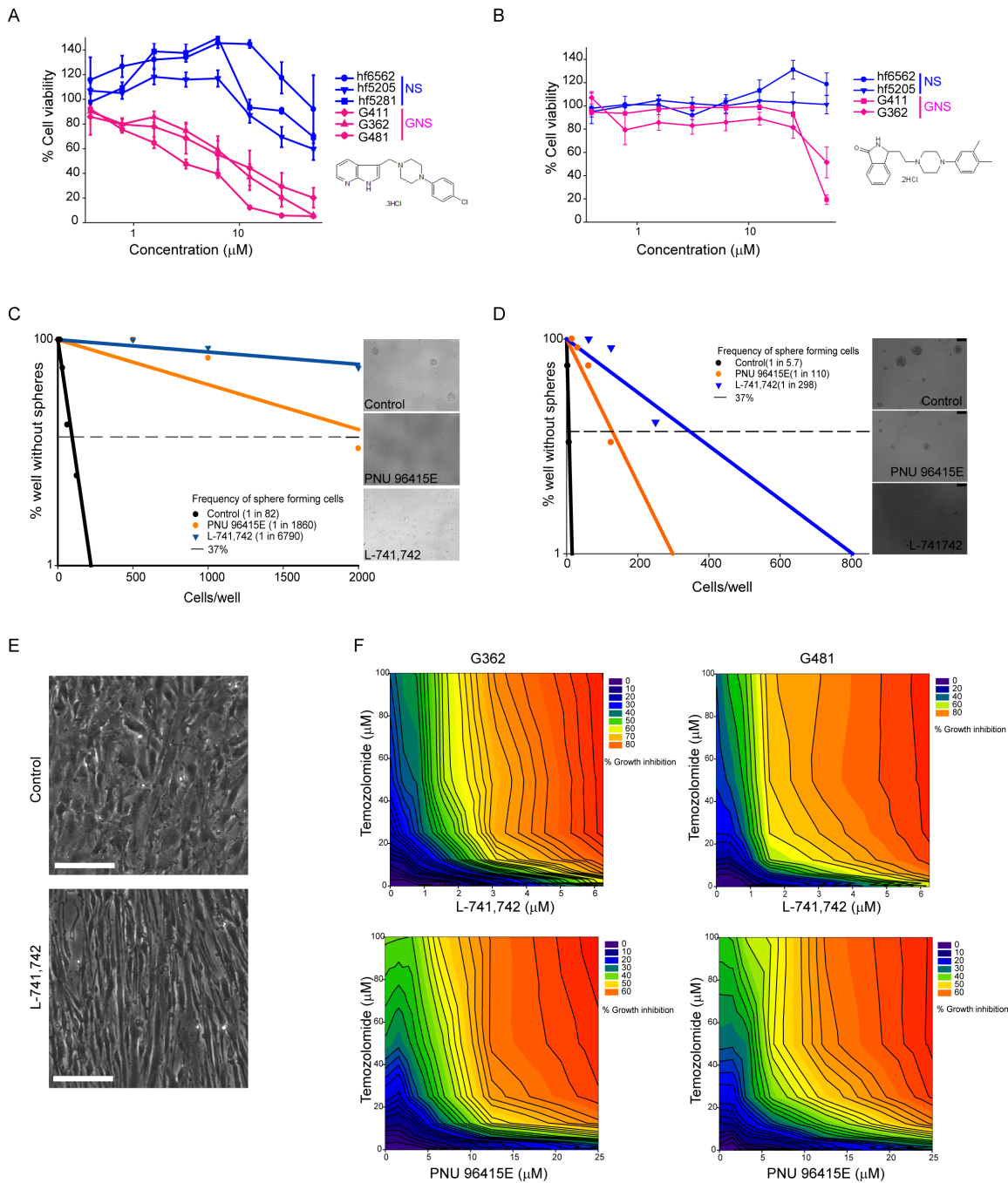


Figure S1, related to Figure 2. DRD4 antagonists are GNS selective, reduce clonogenic cell frequency in primary GBM tumors and are synergistic with TMZ

(A) Percent cell viability of 3 NS and 3 GNS lines upon treatment with dose series of L-745,870 (0.39-50 μM). NS lines $n = 3-11$ mean \pm SEM, GNS lines $n = 3-11$ mean \pm SEM.

(B) Percent cell viability of 2 NS and 2 GNS lines upon treatment with dose series of PD168568 (0.39-50 μM). $n = 3$, mean \pm SEM.

(C, D) Linear regression plot of in vitro LDA for freshly dissociated patient tumor GBM648 (C) and GBM677 (D) treated with L-741,742 (10 μM), PNU 96415E (25 μM) and DMSO. Frequency of sphere forming cells at 95% confidence interval in control DMSO, L-741,742 and PNU 96415E treated cells analyzed using Sigma plot. Representative phase contrast image of neurospheres at day 14 in well seeded with 2000 cells. Scale bar: 100 μm .

(E) Phase contrast image of normal NS (hf5205) treated with L-741,742 (10 μ M) for five days. Scale bar: 100 μ m.

(F) Growth inhibition plot for GNS with TMZ in combination with L-741742 or PNU 96415E.

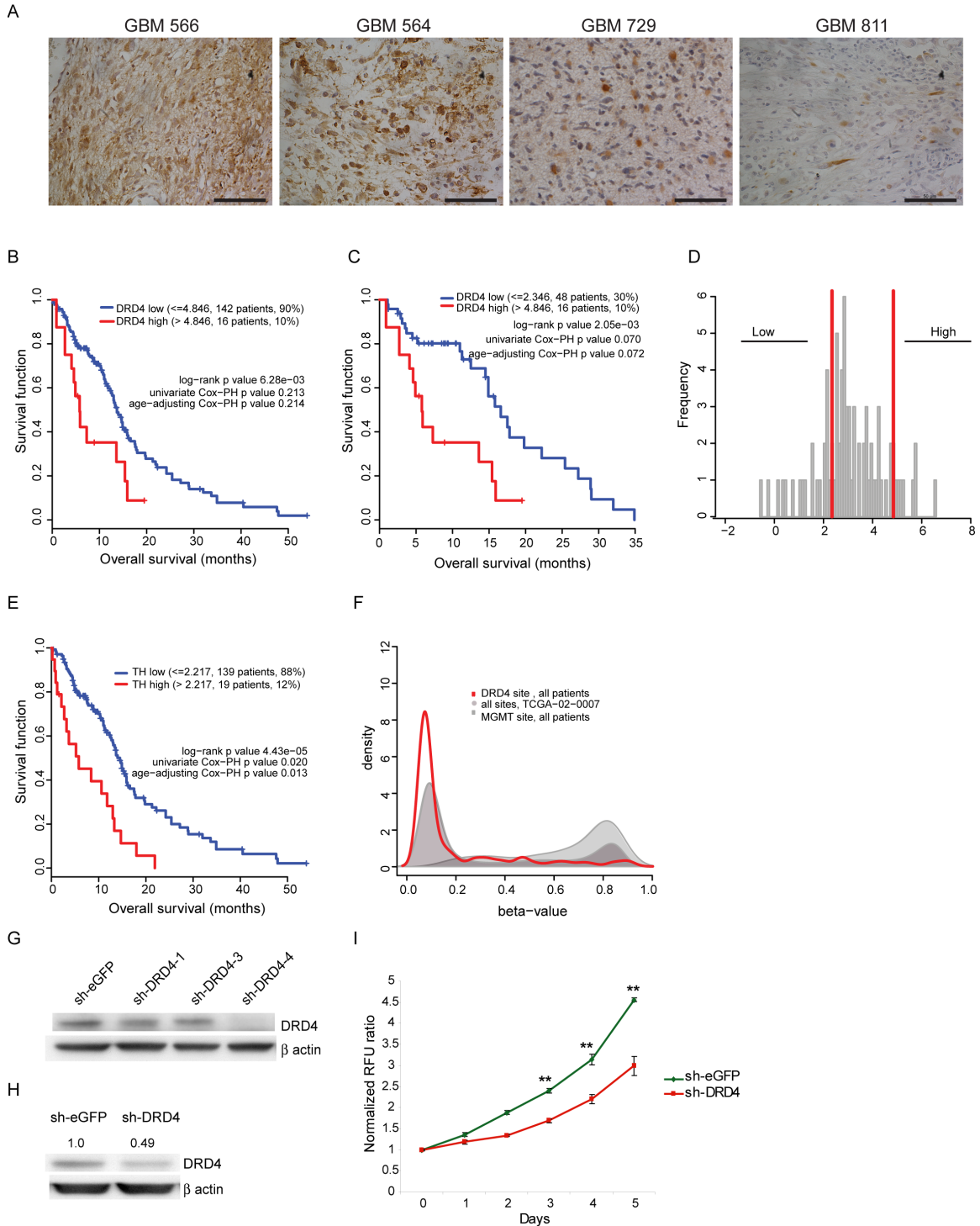


Figure S2, related to Figure 3. DRD4 expression in patient tumor samples, higher DRD4 expression correlates with a worst prognosis, loss of DRD4 suppresses GNS growth.

(A) Immunohistochemistry staining for DRD4 in patient tumor samples. Scale bar: 50 μm .

- (B) Kaplan-Meier overall survival (OS) curve of patients with highest DRD4 expression (RNAseq) compared to remaining low DRD4 population using one cut off.
- (C) Kaplan-Meier OS curve of patient with the highest and lowest DRD4 expression (RNAseq) using two cut offs.
- (D) Histogram representing the DRD4 expression (Log2 value, RNAseq) distribution across all GBM patients and cutoff used for OS curve.
- (E) Kaplan-Meier OS curve of patient showing highest tyrosine hydroxylase (TH) compared to the remaining low expression population using one cut off.
- (F) Density function of the beta-value of DRD4 related CpG sites across all patients. The 2 gray curves are positive control used to localize the positive methylation peak: density function of MGMT related CpG site and density function of all sites for patient TCGA-02-2007.
- (G) Western blot analysis for anti-DRD4 and anti- β actin in GNS (G362) transiently transfected with short hairpins against DRD4 post 72 hr.
- (H) Western blot analysis for anti-DRD4 and anti- β actin in G481 cells transiently transfected with sh-DRD4 and sh-eGFP 72 hr post transfection. Band intensity of DRD4 knockdown expressed relative to control.
- (I) Cell viability assay (Alamar blue) for G481 cells transiently transfected with sh-DRD4 and sh-eGFP measured over 5 days. n = 3, mean \pm SEM. * p value < 0.005, ** p value < 0.0005 unpaired one-tailed t-test.

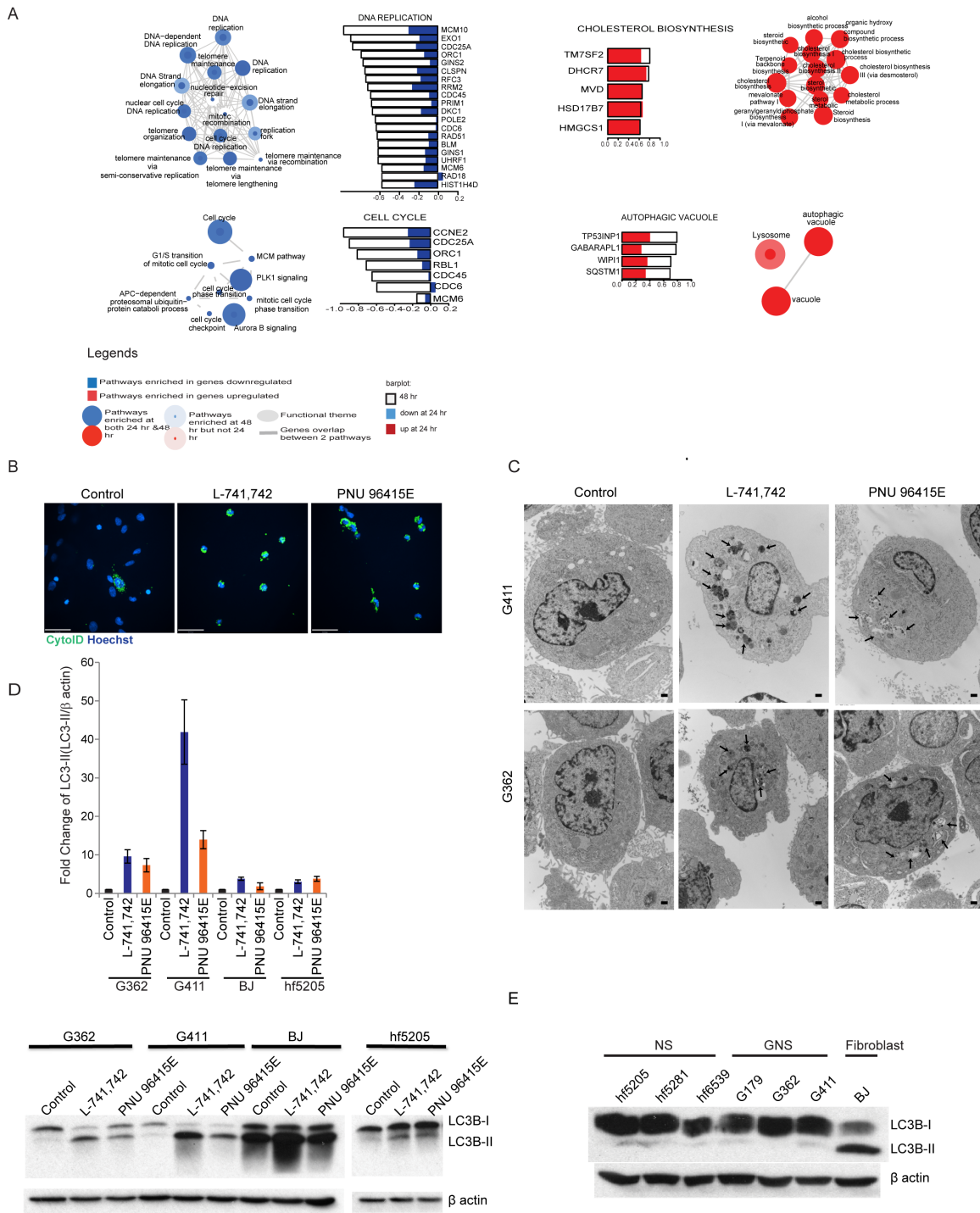


Figure S3, related to Figure 4. Gene expression profile of GNS upon DRD4 antagonism and accumulation of autophagic vacuoles

(A) Blue: Enrichment map showing each gene-set and label contained in ‘DNA replication and Cell Cycle phase / transition’ functional theme from the down regulated map (Figure 4A) (FDR ≤ 0.001). Right: Expression at 24 hr and 48 hr (log FC ≥ -1.5) of genes included in the DNA replication (GO:0006260, FDR =0.0005) and Cell cycle (KEGG:HSA04110, FDR =0.0005) gene-set.

Red: Enrichment map showing each gene-set and label contained in 'Lipid / cholesterol / biosynthesis and Autophagic vacuole / lysosome' theme from the up regulated map (Figure 4A) ($FDR \leq 0.001$). Left: Expression at 24 hr and 48 hr ($\log FC \geq 1.5$) of genes included in the Cholesterol biosynthesis (HUMANCYC%PWY66-5, $FDR = 0.0005$) and autophagic vacuole (GO:0005776, $FDR = 5.0888734E-4$) gene-set.

(B) Fluorescence staining of CytoID-Green (autophagosome marker) in live G411 cells treated with L-741,742 (10 μM) and PNU 96415E (25 μM) at 48 hr treatment. Scale bar: 53 μm .

(C) Transmission Electron Microscopy images showing autophagic vacuoles in a whole cell image of G362 and G411 cells treated with L-741,742 (10 μM) and PNU 96415E (25 μM) at 48 hr. Scale bar: 500 nm.

(D) Western blot analysis for anti-LC3B and anti- β actin across different cell lines, GNS (G362 & G411), NS (hf5205) and Fibroblast (BJ) upon treatment with L-741,742 (10 μM) and PNU 96415E (25 μM) at 48 hr, and quantification of western blots (LC3-II/ β actin). $n = 3$, mean \pm SEM.

(E) Western blot analysis for anti-LC3B and anti- β actin across different cell lines, GNS (G362, G411 & G179), NS (hf5205, hf5281 & hf6539) and Fibroblast (BJ) at basal level.

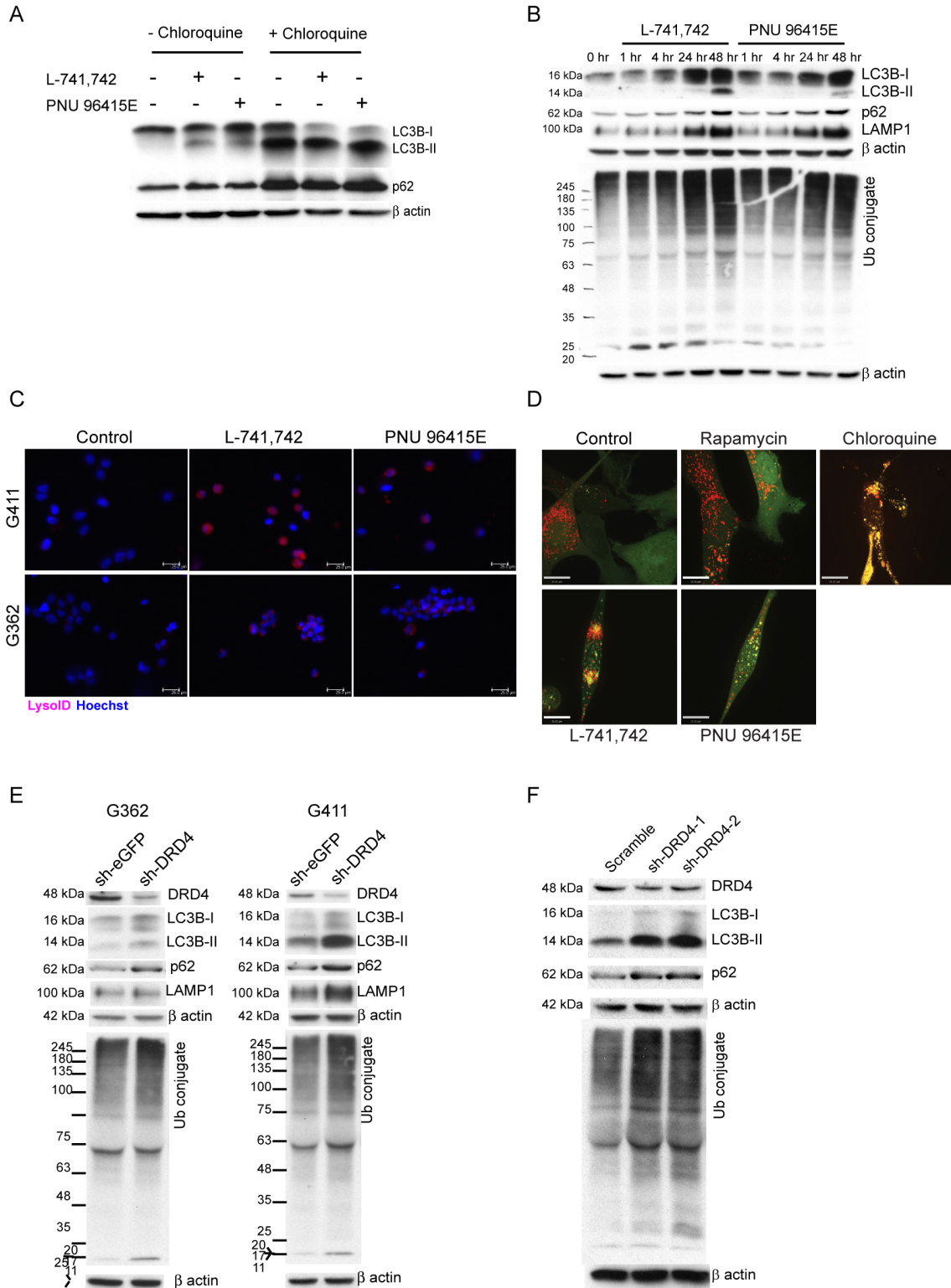


Figure S4, related to Figure 5. DRD4 antagonism causes impaired autophagy-lysosomal degradation pathway in GNS

(A) Western blot analysis for anti-LC3B, anti-p62 and anti- β actin in G362 cells treated with L-741,742 (10 μ M) and PNU 96415E (25 μ M), in the presence and absence of chloroquine (30 μ M) at 48 hr treatment.

(B) Western blot analysis for anti-LC3B, anti-p62, anti-LAMP1 and anti-mono and poly ubiquitinated protein conjugates in G362 cells treated with L-741,742 (10 μ M) and PNU 96415E (25 μ M) at indicated time points.

(C) Fluorescence staining of lysoID-Red (lysosomes marker) in live GNS (G411 and G362) treated with L-741,742 (10 μ M) and PNU 96415E (25 μ M) at 48 hr treatment. Scale bar: 25 μ m.

(D) Confocal analysis of GNS (G411) expressing tandem mRFP-GFP-LC3 reporter treated with Rapamycin (500 nM), Chloroquine (30 μ M), L-741,742 (10 μ M) and PNU 96415E (25 μ M) at 24 hr, red puncta (RFP⁺/GFP⁺/LC3) indicating autolysosome and yellow puncta (RFP⁺/GFP⁺/LC3) indicating autophagosome. Scale bar: 10 μ m.

(E) Western blot analysis for anti-DRD4, anti-LC3B, anti-p62, anti-LAMP1, anti-mono and poly ubiquitinated protein conjugates in GNS, transiently transfected with sh-DRD4 and sh-eGFP (Open Biosystems) post 72 hr.

(F) Western blot analysis for anti-DRD4, anti-LC3B, anti-p62, anti-mono and poly ubiquitinated protein conjugates in G411 cells transiently transfected with an another set of sh-DRD4 from Origene; sh-DRD4-1, sh-DRD4-2, and non-effective scramble shRNA, post 72 hr.

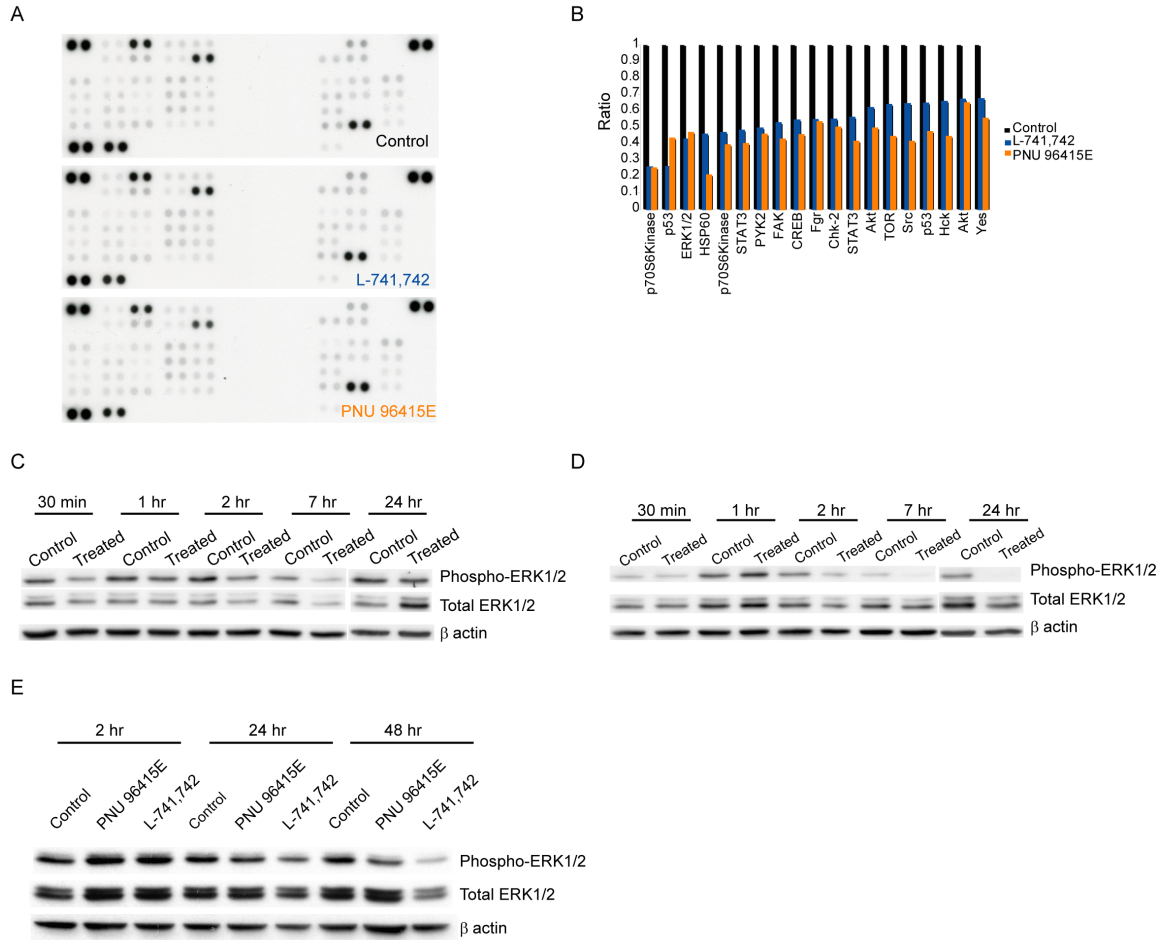


Figure S5, related to Figure 6. Phospho-kinase array reveals suppression of ERK1/2 signaling in GNS upon DRD4 antagonism

(A) A dot blot containing 43 phospho- proteins in duplicates after exposure to lysate of hf5205 cells treated with L-741,742 (10 μ M), PNU 96415E (25 μ M) and DMSO for 24 hr.

(B) Ratio of control versus L-741,742 and PNU 96415E for each phospho-protein that changed upon treatment in GNS (G362 cells) from Figure 6A-B.

(C, D) Western blot analysis for anti-phospho-ERK1/2, anti-ERK1/2 and anti- β actin in hf5205 (C) and G362 (D) respectively treated with L-741,742 (10 μ M) at indicated time points.

(E) Western blot analysis for anti-phospho-ERK1/2, anti-ERK1/2 and anti- β actin in G411 treated with L-741,742 (10 μ M) and PNU 96415E (25 μ M) at indicated time points.

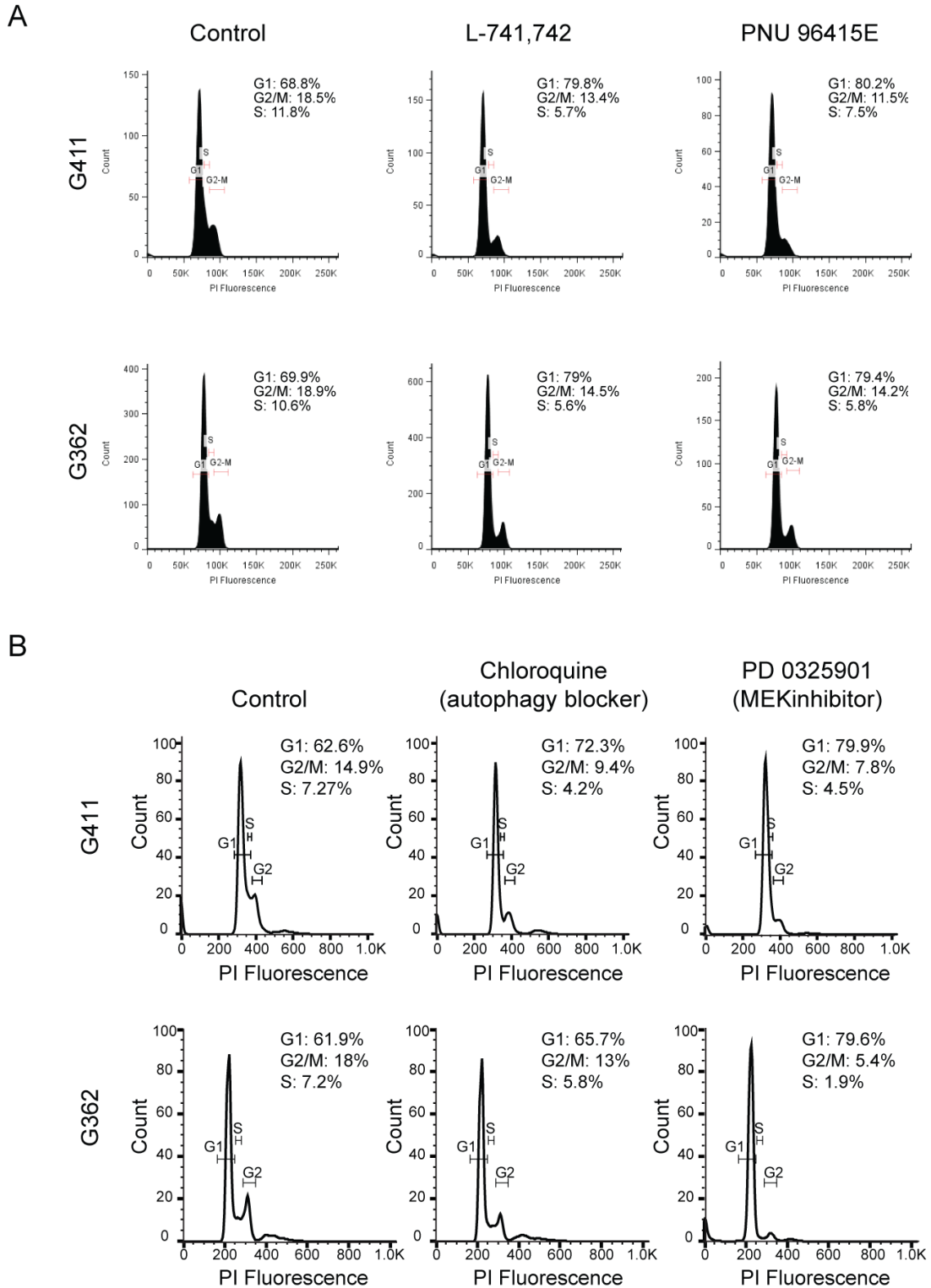


Figure S6, related to Figure 7. DRD4 antagonism cause G₀/G₁ cell cycle arrest

(A) Cell cycle flow cytometry analysis of GNS (G362 and G411) treated with L-741,742 (10 μ M) and PNU 96415E (25 μ M) at 24 hr treatment.

(B) Cell cycle flow cytometry analysis of GNS (G362 and G411) treated with Chloroquine (30 μ M) and PD 0325901 (1 μ M) at 24 hr treatment.

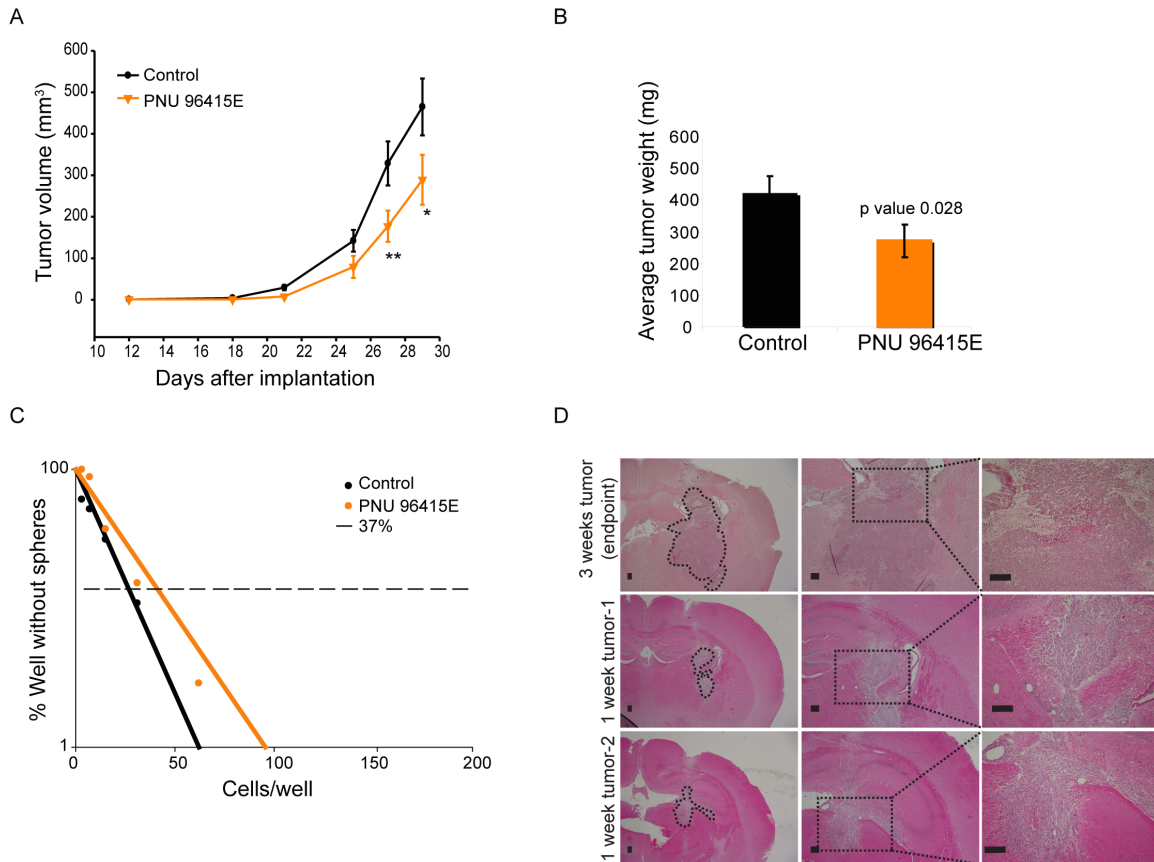


Figure S7, related to Figure 8. DRD4 antagonists reduce GBM xenograft growth in vivo

(A) Growth curve of subcutaneous implanted tumor (G411) over period of time, measured from day 12 after implantation until end point when any tumor reached 17 mm in size. Control n = 16, mean ± SEM and PNU 96415E n = 15, mean ± SEM. **p value-0.014, *p value-0.047, t-test unpaired one-tailed.

(B) Average tumor weight of control and PNU 96415E treated group at the end point. Control n = 16, mean ± SEM, PNU 96415E n = 15, mean ± SEM.

(C) Linear regression plot of in vitro LDA for in vivo treated tumors. Three tumors from three different mice from each group were dissociated and seeded for in vitro LDA. Average of each group was taken for the plot, neurospheres scored for 18 wells (6 wells from each tumors).

(D) H&E staining of intracranial tumor (G362) at week 1 compared to week 3 tumor (end point). Scale bar: 100 μm.

SUPPLEMENTAL EXPERIMENTAL PROCEDURES

Cell culture

BJ fibroblast, Daoy and C8-D1A and U2 OS (ATCC) were maintained in DMEM with 10% FBS.

Chemical Screen

Cells were seeded in laminin coated 384 well plates at a density of 2000 cells per well. Compounds were added at a concentration of 5 μ M and incubated with cells for five days at 37°C. Cell viability was assessed by measuring Alamar Blue incorporation according to the manufacturer's protocol (Invitrogen). Percent growth inhibition was calculated relative to DMSO treated control wells.

Secondary screen / dose response curve

The potency and selectivity of hits from primary screen were tested in 8-point 2-fold dilution series ranging from 50 μ M-0.39 μ M concentrations with additional GNS, NS and fibroblast lines. Experimental conditions were same as in primary screen. IC₅₀ was calculated based on an approximate observed value. Fold selectivity was calculated as IC₅₀ of BJ / IC₅₀ of any GNS with lowest IC₅₀.

Combination / Synergy screen

2000 GNS (G362 and G481) were seeded in 96 well plates and treated with combination of 6-point 2-fold dose series of either L-741,742 (6.25 μ M-0.39 μ M) or PNU 96415E (25 μ M-1.56 μ M) with 10-point 2-fold dose series of TMZ (100 μ M-0.39 μ M) in 60-point combination doses. Cells were incubated with combinations of two drugs for five days and checked for cell viability by Alamar Blue assay. Combination index (CI) plot and CI value was calculated for 5-point dose series in each combination using COMPUSYN. Data points taken for COMPUSYN analysis are TMZ (100, 50, 25, 12.5 and 6.25 μ M) in combination with either L-741,742 (6.25, 3.12, 1.56, 0.78 and 0.39 μ M) or PNU 96415E (25, 12.5, 6.25, 3.12 and 1.56 μ M).

NS differentiation

NS (hf5205 and hf6539) were seeded at 80,000 cells in PLO-laminin coated 10 mm dishes containing coverslips and treated with L-741,742 (4 μ M) in Step-I medium (N2, B27, 5ng/ml FGF) without EGF for first week and replaced with step-II medium (1:1 Neurobasal:Neurocult, B27,1/4 N2) without FGF for next two weeks with L-741,742.

Immunocytochemistry

Cells grown on coverslips were fixed with 4% PFA (or methanol for LC3) and permeabilized with 0.3% Triton X-100, blocked with 5% goat serum, and incubated with primary antibody over night at 4°C, anti-Beta-III tubulin (1:250, MAB1637), anti-VGLUT1 (1:1000, Synaptic system), anti-LC3B at (1:1000, Cell Signaling #3868). Appropriate fluorescent-conjugated secondary antibodies were used at 1:500 for 1 hr at room temperature. Coverslip mounted with fluorescent mounting medium (DAKO) containing DAPI (1:1000) and cells were imaged using Leica light microscope.

In vitro limiting dilution assay (LDA)

Limiting dilution assay was performed as described previously (Tropepe et al., 1999). Primary tumors were dissociated into single cell suspension and seeded in 96 well plate with 10 points-2-fold serial dilution starting from 2000 cells - 4 cells / well, 6 wells for each dilution per plate. Each well was score for neurosphere formation after 14 days of incubation. Percent of wells not containing spheres for each cell density was calculated and plotted against the cells per well and regression lines were plotted and x-intercept value at 0.37 was calculated at 95% confidence interval using Sigma Plot, which gives the number of cells required to form at least one sphere.

Western blots

Western blots were performed using the following antibodies; anti-DRD4 at 1:750 (Millipore# MABN125), anti-phospho-p44/42 MAPK (Erk1/2) at 1:1000 (Cell Signaling), anti-p44/42 MAPK (Erk1/2) at 1:1000 (Cell Signaling), anti- β actin at 1:10,000 (Sigma), anti-LC3B at 1:1000 (Cell Signaling #3868), anti-p62 at 1:1000 (BD Bioscience), anti-LAMP1 at 1:2000 (Developmental Studies Hybridoma Bank), anti-mono and polyubiquitinated protein conjugates (FK2) at 1:1000 (Enzo Life Sciences), anti-phospho-PDGFR β

(Tyr751) at 1:1000 (Cell Signaling), anti-PDGFR β at 1:1000 (Cell signaling), anti-phospho-S6 at 1:2000 (Cell Signaling), anti-S6 at 1:2000 (Cell Signaling).

cAMP assay

cAMP levels were measured with an ELISA-based cAMP assay kit purchased from Cell Signaling (#4439). GNS were seeded overnight in a 96 well plate and treated with forskolin (30 μ M) for 15 minutes, or pretreated with DRD4 agonist A412997 (30 μ M) for 15 minutes followed by forskolin treatment. Cells were lysed and processed as per manufacturer's protocol.

Immunohistochemistry

Primary GBM patient tumor samples or mouse GBM xenograft tumor tissues were fixed overnight in 4%PFA, paraffin embedded and serial sectioned. Sections were deparaffinized and rehydrated through an alcohol gradient to water for antigen retrieval in 10 mM citrate buffer pH 6.0 in a microwave pressure cooker. Endogenous peroxide activity was blocked with 3% (v / v) peroxide in methanol for 15 min at room temperature and nonspecific binding was blocked with 2% (v / v) normal goat or horse serum (vectorlabs) in PBS with 2% (w / v) BSA for 30 min. Primary antibodies; anti-DRD4 at 1:750 (Millipore# MABN125), anti-LC3B at 1:1500 (Cell Signaling #3868), anti-p62 at 1:1000 (BD Bioscience) and anti-mono and polyubiquitinated protein conjugates (FK2) at 1:1000 (Enzo Life Sciences) was incubated overnight at 4°C. Appropriate secondary antibody; biotinylated, avidin-linked peroxidase, DAB (Vectastain Universal Elite ABC kit, Vectorlabs) and Alexa-568 were used to detect binding of the primary antibody. Normal rabbit serum was used for control sections.

Short hairpin construct and transfection

5 μ g of short hairpin targeting DRD4 (RHS4533-EG1815; TRCN0000014453; Thermo Scientific) or control shRNA construct targeting eGFP (RHS4459; Thermo Scientific), and another set of short hairpin against DRD4 from Origene (TL313054A&B) or control non effective scramble shRNA (TR30021) were transfected in 1×10^6 GNS using the Amaxa Nucleofector kit (VPG-1004) and Nucleofector II electroporator (Amaxa Biosystem) according to manufacturer's protocol. After 24 hr post transfection, cells were briefly selected with puromycin for 48 hr and seeded for proliferation assay without selection. Two wells were maintained from each transfection after electroporation; one well lysed to check for knockdown by western blot and the other well seeded for proliferation assay.

Transmission Electron Microscopy

Analysis was performed at Bioimaging facility at Mt Sinai Hospital, Toronto, Canada. Cells were harvested, pelleted and fixed in 2% glutaraldehyde in 0.1M sodium cacodylate buffer, rinsed in buffer, post-fixed in 1% osmium tetroxide buffer, dehydrated in a graded ethanol series followed by propylene oxide, and embedded in EMBED 812 resin. Sections 100 nm thick were cut on an RMC MT6000 ultramicrotome, stained with uranyl acetate and lead citrate and viewed in an FEI Tecnai 20 TEM.

Gene expression profiling

GNS (G362 and G411) were treated with PNU 96415E (25 μ M) for 0 hr (Control) 24 hr and 48 hr and cells lysed for RNA at each time points using RNeasy kit (Qiagen). RNA extracted from the samples was hybridized on Affymetrix Human Gene 1.0 ST arrays using standard protocol (TCAG, Toronto, Ontario, Canada). RMA background correction, quantile normalization and log₂ transformation were applied to the CEL files using the Bioconductor affy package (R 3.0.1, affy package version 1.38.1). Batch correction was applied using ComBat function from sva (3.6.0) and gene annotations were retrieved using hugene10sttranscriptcluster.db (8.0.1). Genes were ranked based on the average log fold change (log FC) of the 2 treated GNS (G411 and G362) at 24 hr or 48 hr to vehicle (0 hr) samples. The data were analyzed using GSEA (Subramanian et al., 2005) with parameters set to 2000 gene-set permutations and gene-sets size between 8 and 500. The gene-sets included in the GSEA analyses were obtained from KEGG, MsigDB-c2, NCI, Biocarta, IOB, Netpath, HumanCyc, Reactome and the Gene Ontology (GO) databases, updated October 14_2013 (<http://baderlab.org/GeneSets>). An enrichment map (version 1.2 of Enrichment Map software (Merico et al., 2010)) was generated for each comparison using enriched gene-sets with a False Discovery Rate < 0.02% and the overlap coefficient set to 0.5.

Phospho-kinase array

A human phospho-kinase antibody array was purchased from R&D systems (Cat# ARY003). This array contains capture antibodies for 43 kinases in duplicate on nitrocellulose membrane. GNS (G362) and NS (hf5205) lines were treated with L-741,742 (10 μ M) and PNU 96415E (25 μ M) along with DMSO control for 24 hr and cells processed according to the manufacturer's protocol. Signal intensity was quantified using ImageJ.

Filipin Staining

Cells were treated as indicated in figure legends and visualized for cholesterol accumulation using filipin staining (Sigma-Aldrich, F9765). After fixing cells with 4% paraformaldehyde, cells were incubated with 1.5mg / ml glycine for 10 min and incubated with 50 mg/ml filipin for 2-3 hr at room temperature. Images were captured using Quorum spinning disc confocal microscopy.

Apoptosis assay

Cells were seeded at 2500 cells / well in 96 well clear bottom black plates and treated with compounds as indicated in figure legends. Apoptosis assay was performed using Apo-ONE Homogenous Caspase3 / 7 assay kit (Promega-G7790) as per protocol and plate measured for fluorescence after 4 hr incubation.

Lysosomal and autophagosomal staining

LysoID-Red and CytoID-Green kit was purchased from Enzo Life Sciences. LysoID and CytoID were diluted 1000X in serum free medium and incubated with cells grown on coverslips after the indicated treatment for 30 min at 37°C, washed and visualized immediately by confocal microscope.

Cell cycle analysis

Cells were fixed in 70% ice-cold ethanol at -20°C overnight. Cells were then washed in PBS and resuspended in 500 μ l of PBS containing 30 μ g/ml Propidium Iodide (Sigma) and 100 μ g/ml RNase A and incubated for 30 min at room temperature. DNA content was determined by flow cytometry.

Statistical analysis

Kaplan Meier curves were generated and analyzed using Prism 6.0 (GraphPad Inc.) or Excel (Microsoft, Inc.) and XLSTAT (Addinsoft, Inc.). A log rank test was used to compare groups (p values as in Figure 8E, 8F). The frequency of deaths or censorships was assessed using a Fisher's exact test (Prism 6.0). A Cox proportional hazard model was used to compare the effects of TMZ dosage (12.5 mg/kg or 25 mg/kg) or L-741,742 dosage (0 or 25 mg/kg) as independent quantitative variables for the data in Figure 8F, and only L-741,742 treatment significantly affected survival (hazard ratio 0.960, p= 0.027). Thus, whether used alone (Figure 8E) or in combination with TMZ (Figure 8F), L-741,742 treatment was the only variable significantly associated with an improvement in survival.

SUPPLEMENTAL REFERENCES

Merico, D., Isserlin, R., Stueker, O., Emili, A., and Bader, G. D. (2010). Enrichment map: a network-based method for gene-set enrichment visualization and interpretation. *PloS one* 5, e13984.

Subramanian, A., Tamayo, P., Mootha, V. K., Mukherjee, S., Ebert, B. L., Gillette, M. A., Paulovich, A., Pomeroy, S. L., Golub, T. R., Lander, E. S., and Mesirov, J. P. (2005). Gene set enrichment analysis: a knowledge-based approach for interpreting genome-wide expression profiles. *Proceedings of the National Academy of Sciences of the United States of America* 102, 15545-15550.

Tropepe, V., Sibilio, M., Ciruna, B. G., Rossant, J., Wagner, E. F., and van der Kooy, D. (1999). Distinct neural stem cells proliferate in response to EGF and FGF in the developing mouse telencephalon. *Developmental biology* 208, 166-188.